Nonlinear Analysis of the Wein Bridge Oscillator Circuit

Ronak Roy
Department of Mechanical Engineering
Massachusetts Institute of Technology
Cambridge, MA, U.S.A
ronakroy@mit.edu

I. Motivation

The three basic elements of circuits are the resistor, capacitor, and inductor. These are two-terminal devices, of which the state can be captured by voltage v, the measure or electrical potential *across* the terminals, and current i, the measure of the flow of electricity *through* the component.

From first principles, one can derive the constitutive laws for a resistor (1), capacitor (2), and inductor (3) with resistance R, capacitance C, and inductance L, respectively [1].

$$v = Ri \tag{1}$$

$$\frac{dv}{dt} = \frac{1}{C}i \tag{2}$$

$$v = L\frac{di}{dt} \tag{3}$$

One strength of circuit analysis is the high degree of linearity that these basic components exhibit when measured experimentally, accurately capturing almost all current-voltage dynamics. As such, analog electronics engineers have been able to design circuits for signal processing, power generation, radio transmission, closed-loop feedback with remarkable model-to-real transfer. In all of these domains, it is natural to use frequency-domain analysis (specifically through the Laplace transform)–the linear components have very predictable input/output gain and phase shift dynamics with respect to sinusoids.

As such, in the design of circuits and development of electrical components, one powerful experimental tool is sinusoidal steady-state analysis, in which constant amplitude sine waves are input into a component or system, and the gain and phase shift are calculated. To achieve this, a means of generating low-distortion sinusoids that is resistant to loading (i.e. the sine wave being changed by the components that use it as an input) is important.

While sinusoids can come out of linear systems, generating stable, deterministic sinusoids requires nonlinear dynamics. In this project, we will investigate these nonlinearities in one of the original high-quality sine wave generators: the Wein bridge oscillator.

II. Linear Circuit

A. Linear Analysis

The Wein bridge oscillator circuit is shown below in Fig. 1 [2]. The oscillator circuit relies on two main principles to create and sustain oscillations.

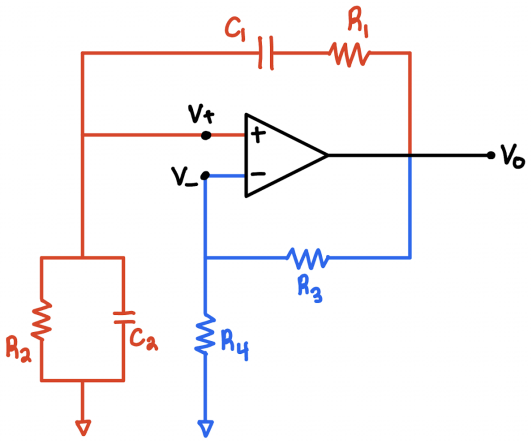

Fig. 1: The Wein bridge oscillator circuit schematic.

The first part is the Wein bridge circuit, highlighted in red. To analyze the circuit, we use the method of complex impedances, with constitutive laws described in (4) and (5) [3].

$$v = Ri \Leftrightarrow V(s) = RI(s) \implies Z_R = R \tag{4}$$

$$\frac{dv}{dt} = \frac{1}{C}i \Leftrightarrow V(s) = \frac{1}{sC}I(s) \implies Z_C = \frac{1}{sC} \tag{5}$$

Using this transform and the principle of *voltage dividers* [4], we can calculate the *s-domain transfer function* that represents the how an input signal (in this case, v_o) is transformed to an output signal (in this case, v_+) by a system

(in this case, the Wein bridge).

$$\begin{aligned}\frac{V_+}{V_o}(s) &= \frac{\frac{1}{1/R_2 + 1/\frac{1}{sC_2}}}{R_1 + \frac{1}{sC_1} + \frac{1}{1/R_2 + 1/\frac{1}{sC_2}}} \\ &= \frac{sR_2C_1}{s^2R_1C_1R_2C_2 + s(R_1C_1 + R_2C_2 + R_2C_1) + 1} \\ &= \frac{s\tau_{21}}{s^2\tau_1\tau_2 + s(\tau_1 + \tau_2 + \tau_{21}) + 1} \end{aligned} \tag{6}$$

The triangular component in the middle is known as an operational amplifier (op-amp), which is an active circuit component that outputs a voltage proportional to the difference of the input voltage, as per (7).

$$v_o = A(v_+ - v_-) \Leftrightarrow V_o(s) = A(V_+(s) - V_-(s)) \tag{7}$$

Unlike passive (capacitors and inductors) and dissipative (resistors) components, op-amps are able to input energy into a system. When an op-amp is connected in a *negative feedback* configuration, we get:

$$\frac{V_-}{V_o}(s) = \frac{R_4}{R_3 + R_4} = \frac{1}{G} \tag{8}$$

We now combine the Wein bridge (6), feedback (8), and op-amp (7) dynamics to determine the overall system dynamics, and transform back into the time domain.

$$\begin{aligned} V_o &= A(V_+ - V_-) \\ 0 &= V_o\left(s^2\tau_1\tau_2 + s\left(\tau_1 + \tau_2 + \tau_{21} - \frac{GA}{G+A}\tau_{21}\right) + 1\right) \\ &= \tau_1\tau_2\ddot{v_o} + \left(\tau_1 + \tau_2 + \tau_{21} - \frac{GA}{G+A}\tau_{21}\right)\dot{v_o} + v_o. \end{aligned} \tag{9}$$

As we can see, the overall circuit behaves as a damped harmonic oscillator, which takes normalized form

$$0 = \frac{1}{\omega_n^2}\ddot{x} + \frac{2\zeta}{\omega_n}\dot{x} + x.$$

It oscillates with damped frequency $\omega_d = \omega_n\sqrt{\zeta^2 - 1}$ and has amplitude that exponentially decays according to $e^{-\omega_n\zeta t}$. When constructing this circuit, we will use a 741 op-amp, which has open-loop gain $A = 200000$.

To make our system oscillate at a constant amplitude, we must make $\zeta = 0 \implies$

$$\begin{aligned} 0 &= \tau_1 + \tau_2 + \tau_{21} - \frac{G_*A}{G_* + A}\tau_{21} \\ &= \tau_1 + \tau_2 + \tau_{21} - G_*\tau_{21} \text{ for } A \gg G_* \\ \implies G_* &= \frac{\tau_1 + \tau_2}{\tau_{21}} + 1 \end{aligned} \tag{10}$$

One straightforward way to achieve this is to match τ_1, τ_2, and τ_{21}, which would then require $G_* = 3 \implies R_3 = 2R_4$.

B. Experimental Validation

Given this seemingly simple linear solution, we construct the circuit. Since the circuit is fully linear, the oscillation amplitude is a function of the initial conditions–we'll trust electrical noise to allow for some oscillations, and focus on the oscillator's frequency. The constructed circuit shown in Fig. 2 uses the nominal component values shown in Table I.

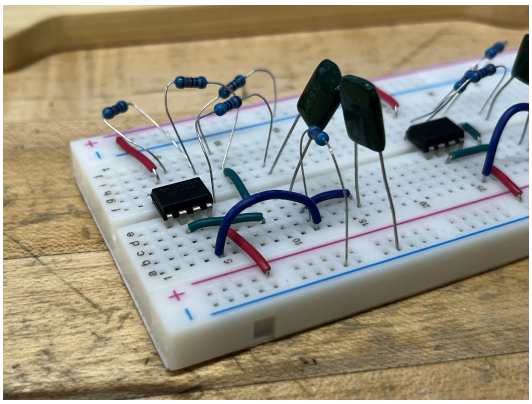

Fig. 2: Constructed Wein bridge oscillator circuit.

TABLE I: Nominal component values in circuit A1.

component	value
R_1	47 kΩ
C_1	68 nF
R_2	47 kΩ
C_2	68 nF
R_3	20 kΩ
R_4	10 kΩ

These components should produce oscillations of frequency 49.8Hz. Using an oscilloscope, we measure the voltage v_o. As we can see in Fig. 3, the frequency is approximately correct, but the amplitude is increasing.

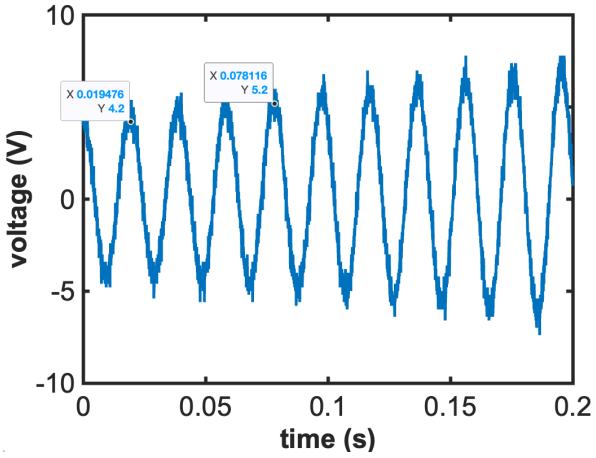

Fig. 3: Recorded experimental data for circuit A1. We measure oscillation frequency $\frac{3}{.0781-.0195} = 51.2$Hz.

When we use a digital multimeter to measure the actual component values, we see deviations in the actual value of each component. Table II shows these measurements.

TABLE II: Nominal versus measured component values in circuit A1.

component	nominal value	measured value
R_1	47 kΩ	46.54 kΩ
C_1	68 nF	68.12 nF
R_2	47 kΩ	46.14 kΩ
C_2	68 nF	65.93 nF
R_3	20 kΩ	19.69 kΩ
R_4	10 kΩ	9.875 kΩ

With these actual values, we get damping ratio $\zeta = \frac{\omega_n}{2}(\tau_1 + \tau_2 + \tau_{21} - G\tau_{21}) = -0.009$, which, while small, generates exponential growth. Plotting the model alongside the experimental data in Fig 4 shows excellent alignment.

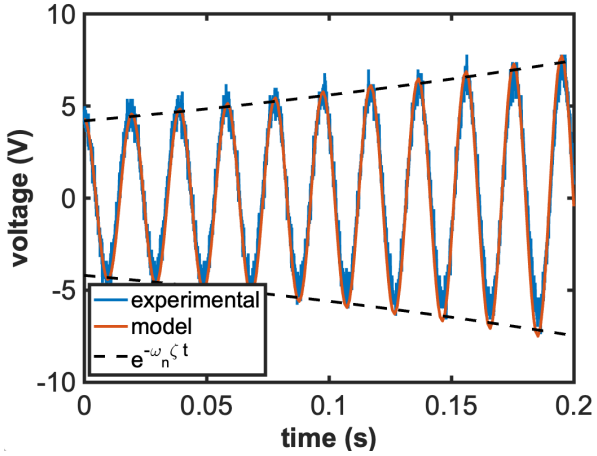

Fig. 4: Experimental, recorded data for circuit A1 compared with the linear model using measured component values.

This experimental result reveals a massive caveat with the linear circuit construction. For marginal stability (the type that generates oscillations), the component values must be exactly matched to each other to cancel out oscillations. In practice, commodity resistors and capacitors are not nearly precise enough to guarantee this.

Finally, to further validate the accuracy of our purely linear model, we reduce G by making $R_3 = 14.77k\Omega$ ($15k\Omega$ nominal) and $R_4 = 8.081k\Omega$ ($8k\Omega$ nominal), yielding a $\zeta = .075$. The experimental results are shown in comparison to the model in Fig. 5.

III. "Unintentional" Nonlinearities

Obviously, in a physical system, exponential growth cannot occur forever. We expect the system's growth to somehow be limited. A purely linear system can only have one fixed point, which, for this system, is at the origin. Thus, any limitation that bounds growth must be a nonlinearity.

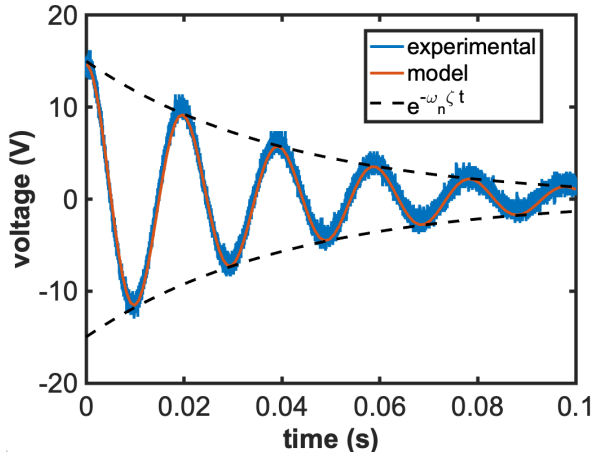

Fig. 5: Experimental, recorded data for circuit A3 (A1 with lesser G) compared with the linear model using measured component values.

A. Saturation

In the case of an op-amp, this nonlinearity is saturation. The op-amp is only capable of outputting the voltage that is within the bounds of its supply voltage, after which it saturates [5], as shown in Fig 6.

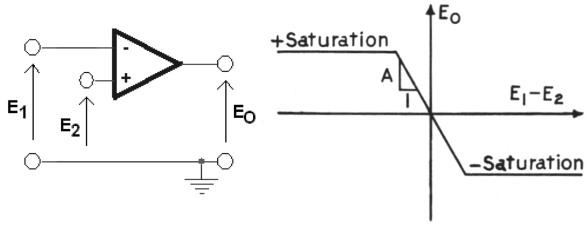

Fig. 6: Saturation behavior of an op-amp [5].

From our canonical linear system dynamics in 9, we can decompose into the 2D system in (11) with state vector $\vec{v} = [v_o \ \dot{v}_o]^T$

$$\begin{cases} \dot{v}_o = \dot{v}_o \\ \ddot{v}_o = -\dfrac{(\tau_1 + \tau_2 + \tau_{21} - G\tau_{21})\dot{v}_o + v_o}{\tau_1\tau_2} \end{cases} \tag{11}$$

To include the saturation behavior in our model, we impose a "filter" on $\dot{v}_o$. During saturation, the op-amp output voltage is only permitted to become lesser in magnitude. Additionally, if (via some initial conditions) the op-amp output voltage is pulled beyond its saturation voltage, the internal dynamics will cause the voltage to rapidly decay towards saturation voltage. One caveat with this model is that the system state is bounded–if the output voltage is pulled too far beyond saturation, the silicon of the op-amp will permanently break

down and fry the part. Assuming we do not operate in that regime, we develop the filter (12)

$$s(x) = x\left(1 - \sigma(-(x - X_l))\sigma(-x) - \sigma(x - X_u)\sigma(x)\right) + 500\left((X_l - x)\sigma(-(x - X_l)) + (X_u - x)\sigma(x - X_u)\right) \tag{12}$$

where:

$\sigma(x)$ = smooth step function $\frac{1}{1+e^{-100x}}$
X_l = lower saturation bound
X_u = upper saturation bound

We apply this filter to give us new, nonlinear system dynamics (13).

$$\begin{cases} \dot{v}_o = s(\dot{v}_o) \\ \ddot{v}_o = -\dfrac{(\tau_1 + \tau_2 + \tau_{21} - G\tau_{21})\dot{v}_o + v_o}{\tau_1\tau_2} \end{cases} \tag{13}$$

To analyze this system, we perform a similar parametrization as the linear analysis, using the gain $G = \frac{R_3}{R_4} + 1$ as our parameter. It is still true that the critical parameter value $G_* = 1 + \dfrac{\tau_1 + \tau_2}{\tau_{21}}$ makes the system linearly marginally stable, i.e. generates infinitely many closed orbits. For $G < G_*$, the fixed point at the origin is stable. Finally, for $G > G_*$ case, the system exhibits behavior that only exists due to the saturation nonlinearity–tending to a limit cycle defined by the saturation bounds. Thus, we can see that with respect to op-amp feedback gain G, this 2D system exhibits a **degenerate Hopf bifurcation**, which is shown in the phase plots in Fig 7.

B. Experimental Validation

We construct a third version of circuit A, using the component values listed in Table III. This circuit has $G_* = 2.9765$ and $G = 3.1792$, putting it in the stable limit cycle regime.

TABLE III: Nominal versus measured component values in circuit A3.

component	nominal value	measured value
R_1	47 kΩ	46.54 kΩ
C_1	68 nF	68.12 nF
R_2	47 kΩ	46.14 kΩ
C_2	68 nF	65.93 nF
R_3	22 kΩ	21.52 kΩ
R_4	10 kΩ	9.875 kΩ

We can see from the experimental, time-series data in Fig 8 that the system obeys the linear, exponential growth initially, but then crashes into the predicted saturation bounds. The phase portrait in Fig 9 shows that the model accurately predicts the approach to the limit cycle. To obtain the derivative of output voltage, we use a filtered, discrete differentiation scheme. Unfortunately, the low digital resolution of the scope makes the raw, differentiated signal appear heavily quantized, necessitating heavy filtering. This results in softened corners, since the transitions between not-saturated and saturated are rather sharp.

To effectively evaluate the accuracy of our model with respect to the limit cycle, we use the time averaging functionality of the scope, which averages multiple cycles of periodic waveforms taken over time. This is a common method of increasing resolution of oscilliscope readings, since so long as the underlying signal is truly periodic, the noise is removed without adding the artifacts of low-pass filtering a single cycle. This average data is showed in Fig 10 demonstrates remarkably accurate modelling.

IV. Nonlinear Feedback

However, the goal with an oscillator circuit is often to generate sinusoids with minimal distortion and deterministic amplitude–using the saturation of the op-amp to limit the amplitude is not good practice. To generate a stable, isolated periodic orbit, we need to introduce a nonlinearity in our circuit dynamics.

One natural place to introduce this nonlinearity is in the feedback gain G. In the linear circuit, it is constant, but to make a stable limit cycle, we would want to make it a function of the output voltage. Intuitively, we would want to increase the gain G when the amplitude is too low and decrease G when the amplitude is too high, thus stabilizing the amplitude of oscillations.

A. Incandescent Light Bulbs

Historically, the first nonlinear feedback mechanism used to stabilize the Wein bridge oscillator is a light bulb [6]. A lightbulb can be modelled as a temperature dependent resistor, which follows the constitutive law [7]

$$R(T) = R_0(1 + \alpha(T - T_0)) \tag{14}$$

where:

T = temperature (K)
α = temperature coefficient of resistance (Ω/K)
T_0 = room temperature (measured to be 295K)
R_0 = resistance (Ω) measured at room temperature

Additionally, we model the energy transfer using the First Law of Thermodynamics [8]:

$$mc\dot{T} = \frac{v_R^2}{R(T)} - Q(T). \tag{15}$$

where:

m = mass of filament (kg)
c = specific heat of filament (J/kgK)
v_R = voltage (V) across resistor
Q = heat emitted by bulb (W)

Since the lightbulb gets white-hot, we can assume the heat emitted by the bulb is largely due to radiation, which follows the law [8]:

$$Q(T) = \epsilon\sigma A_s(T^4 - T_0^4). \tag{16}$$

where:

ϵ = thermal emissivity coefficient
σ = Steffan-Boltzmann constant (W/m$^2K^4$)
A_s = surface area of filament (m^2)

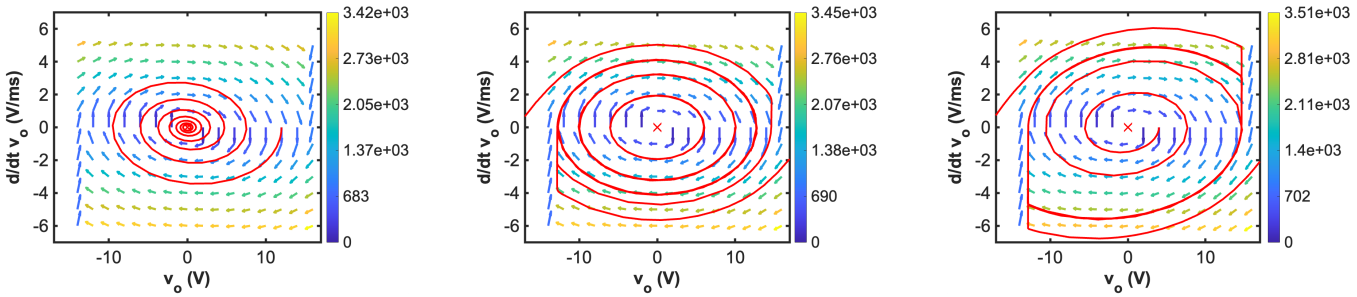

(a) $G < G_*$ (b) $G = G_*$ (c) $G > G_*$

Fig. 7: Phase portraits for different values of G.

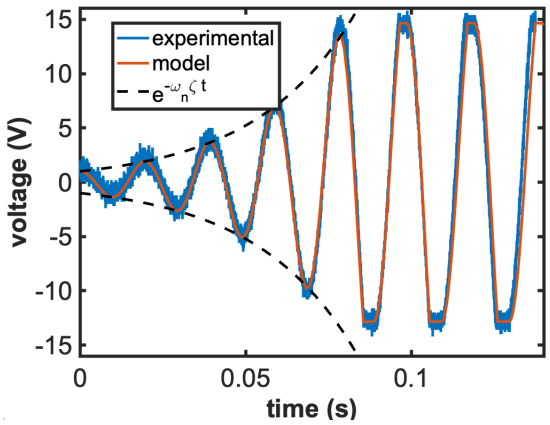

Fig. 8: Time-series, recorded experimental data for circuit A3, compared with model integrated using MATLAB's built-in stiff system solver.

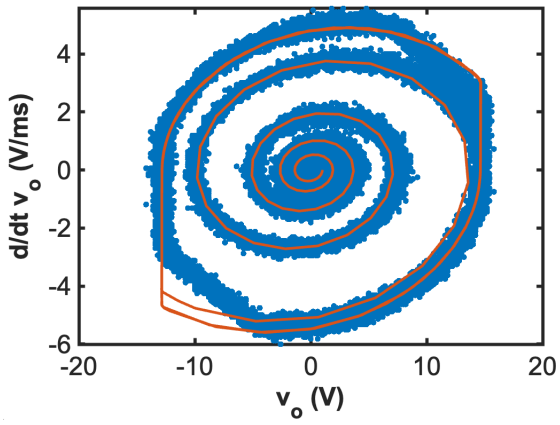

Fig. 9: Phase-plane, recorded experimental trajectory for circuit A3, compared with model integrated using MATLAB's built-in stiff system solver.

B. Lightbulb-driven Nonlinear Feedback

If we replace R_4 in the oscillator circuit with the lightbulb, which has resistance $R(T)$, we get that

$$v_r = v_- = \frac{R(T)}{R_3 + R(T)} v_o \tag{17}$$

$$G(T) = 1 + \frac{R_3}{R(T)}. \tag{18}$$

Altogether, we get the new dynamic equations of this system for system state $\vec{x} = [v_o \ \dot{v}_o \ T]^T$:

$$\begin{cases} \dot{v}_o = \dot{v}_o \\ \ddot{v}_o = -\dfrac{(\tau_1 + \tau_2 + \tau_{21} - G(T)\tau_{21})\dot{v}_o + v_o}{\tau_1 \tau_2} \\ \dot{T} = \dfrac{1}{mc}\left(\dfrac{R(T)}{(R_3 + R(T))^2} v_o^2 - Q(T)\right). \end{cases} \tag{19}$$

While we could analyze and simulate the full system, one important detail is that we do not actually care about the entirety of the system state. Particularly, we have not perturbed the voltage oscillator dynamics except for with temperature-dependent gain. Thus, we still expect damped harmonic oscillations–so, we can transform from voltage and voltage derivative $v_o, \dot{v}_o$ to voltage amplitude and phase A, ϕ space by

$$v_o = Ae^{-\omega_n \zeta t} \sin(\omega_d t + \phi(t)).$$

Additionally, for the purposes of power dissipation, we can use root-mean-squared voltage $< v_o >= \frac{1}{\sqrt{2}} A$. Using this transformation, we can get reduced system dynamics:

$$\begin{cases} \dot{A} = -\zeta(T)\omega_n A \\ \dot{T} = \dfrac{1}{mc}\left(\dfrac{R(T)}{(R_3 + R(T))^2}\dfrac{A^2}{2} - Q(T)\right) \end{cases} \tag{20}$$

where, as with our linear system dynamics:

$$\omega_n = \frac{1}{\sqrt{\tau_1 \tau_2}}; \ \zeta(T) = \frac{\omega_n}{2}(\tau_1 + \tau_2 + (1 - G(T))\tau_{21}),$$

and the actual voltage signal to be a sine wave with damped frequency $\omega_d = \omega_n \sqrt{1 - \zeta^2}$.

We see one trivial fixed point at $A_0 = 0$ and T_0. Additional fixed points, unfortunately, cannot be computed analyticallys.

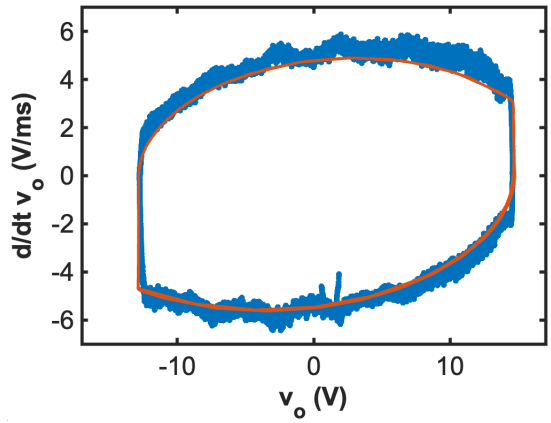

Fig. 10: Phase-plane, recorded experimental trajectory for circuit A3, collected using oscilloscope averaging, and compared with model integrated using MATLAB's built-in stiff system solver.

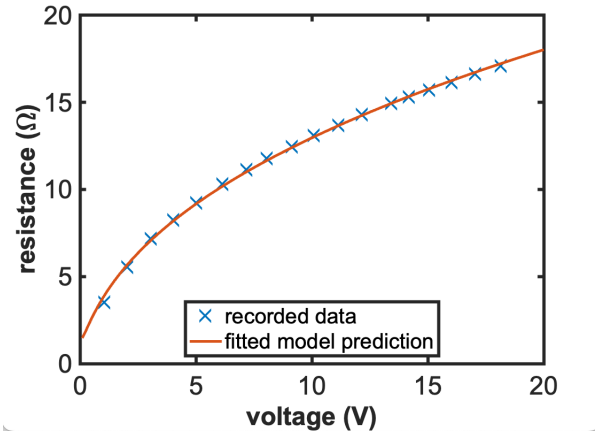

Fig. 11: Steady-state resistance measured at various applied voltages for the lightbulb.

We will later turn to numerical solvers to calculate fixed points.

We use MATLAB symbolic solver to differentiate and obtain the Jacobian:

first column:

$$\begin{bmatrix} -\omega_n^2(\tau_1+\tau_2-\frac{R_3\tau_{21}}{R_0(\alpha(T-T_0)+1)})/2 \\ \frac{AR_0(\alpha(T-T_0)+1)}{mc(R_3+R_0(\alpha(T-T_0)+1))^2} \end{bmatrix}$$

second column:

$$\begin{bmatrix} -\frac{AR_3\alpha\tau_{21}\omega_n^2}{2R_0(\alpha(T-T_0)+1)^2} \\ \left(-\frac{(4T_s^3-(A^2R_0\alpha)}{(2(R_3+R_0(\alpha(T-T_0)+1))^2)}+\frac{(A^2R_0^2\alpha(\alpha(T-T_0)+1))}{(R_3+R_0(\alpha(T-T_0)+1))^3}\right)\frac{1}{mc} \end{bmatrix}$$

C. Lightbulb Coefficient Determination

The exact constants in the light bulb's model $(R_0, \alpha, \epsilon, m, c, A_s)$ are constrained to the values that commercially available lightbulbs have–I purchased a random lightbulb from Amazon that operated in our voltage range. Using a multimeter, we can easily determine $R_0 = 1.35\Omega$. To experimentally determine some of these coefficients, we can turn to steady-state analysis. If we pass in a constant voltage, the temperature will eventually equilibrate ($\dot{T} = 0$). Experimentally, this happens remarkably quickly, indicating that mc is relatively small.

Thus, upon gathering $v_R - R$ data at a range of steady-stave voltages, we can fit α, and ϵA_s, since only these parameters are present in $\dot{T} = 0$. Fig 11 shows the experimentally measured steady-state data and the fit, which has $R^2 > 99\%$. The fit gives $\alpha = .0132$ and $\epsilon A_s = 1.692 \cdot 10^{-4}$.

D. Fixed Point/Linear Stability/Bifurcation Analysis

In constructing this circuit, we will use the same values of R_1, R_2, C_1, C_2. However, we will instead use an OPA548 op-amp, which supports higher saturation voltage (30V) and more output current (which is neccessary to power a light bulb).

We still have one undetermined coefficients: mc, which represents the thermal mass of the lightbulb's filament. The larger mc, the more time it takes for the filament to heat up, and the slower the resistance changes. Upon varying mc, as seen in Fig 12, the fixed points' locations do not appear to be changed. Instead, it "reduces" the stability by invoking more orbiting the stable fixed point, but always appears to be stable. This makes sense–mc simply scales the temperature dynamic equation. We wouldn't expect it to make the system go unstable for any reasonable magnitude of mc (lightbulb filaments have, by design, very small thermal masses).

We now turn to the actual tunable parameter: R_3. As can be seen in Fig 13, R_3 decides the location of the fixed point with nonzero-amplitude. Intuitively, this makes sense: similarly to the linear circuit, there is a "critical" value of $G(T) = G_*$ value in which the system reaches steady state. Changing R_3 changes the steady-state $R(T)$ needed to achieve this critical gain, which in turn changes the steady state sine wave amplitude that creates the temperature that gives the correct $R(T)$.

Using the Jacobian calculated earlier, we actually find a linear stability analysis yield an eigenvalue that is zero for all of the apparently stable equilibrium points. From the phase portraits, we can see that the system always has a stable equilibrium and no limit cycles.

Additionally, as seen in the bifurcation diagram in Fig 14, there is a critical $R_{3,c} = 2.65\Omega$; at lesser R_3, the non-zero stable equilibrium goes out of existence and the zero equilibrium becomes stable. Physically, this represents R_0 being too high to allow the system to oscillate at all, i.e. $G(T_0) < G_c$.

E. Hardware Validation

To stay within physical limitations, we choose $R_3 = 20.05\Omega$ (20Ω nominal), which gives us a predicted amplitude

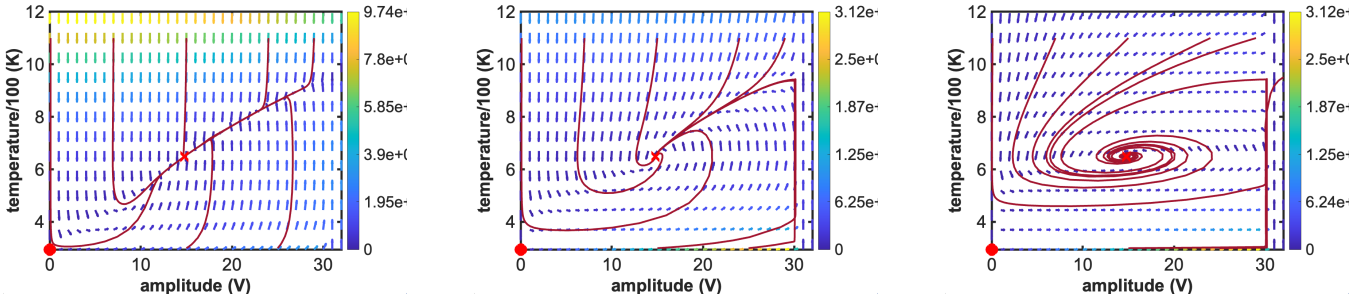

(a) $mc = 10^{-6}$ (b) $mc = 10^{-5}$ (c) $mc = 10^{-4}$

Fig. 12: Phase portraits for different values of mc.

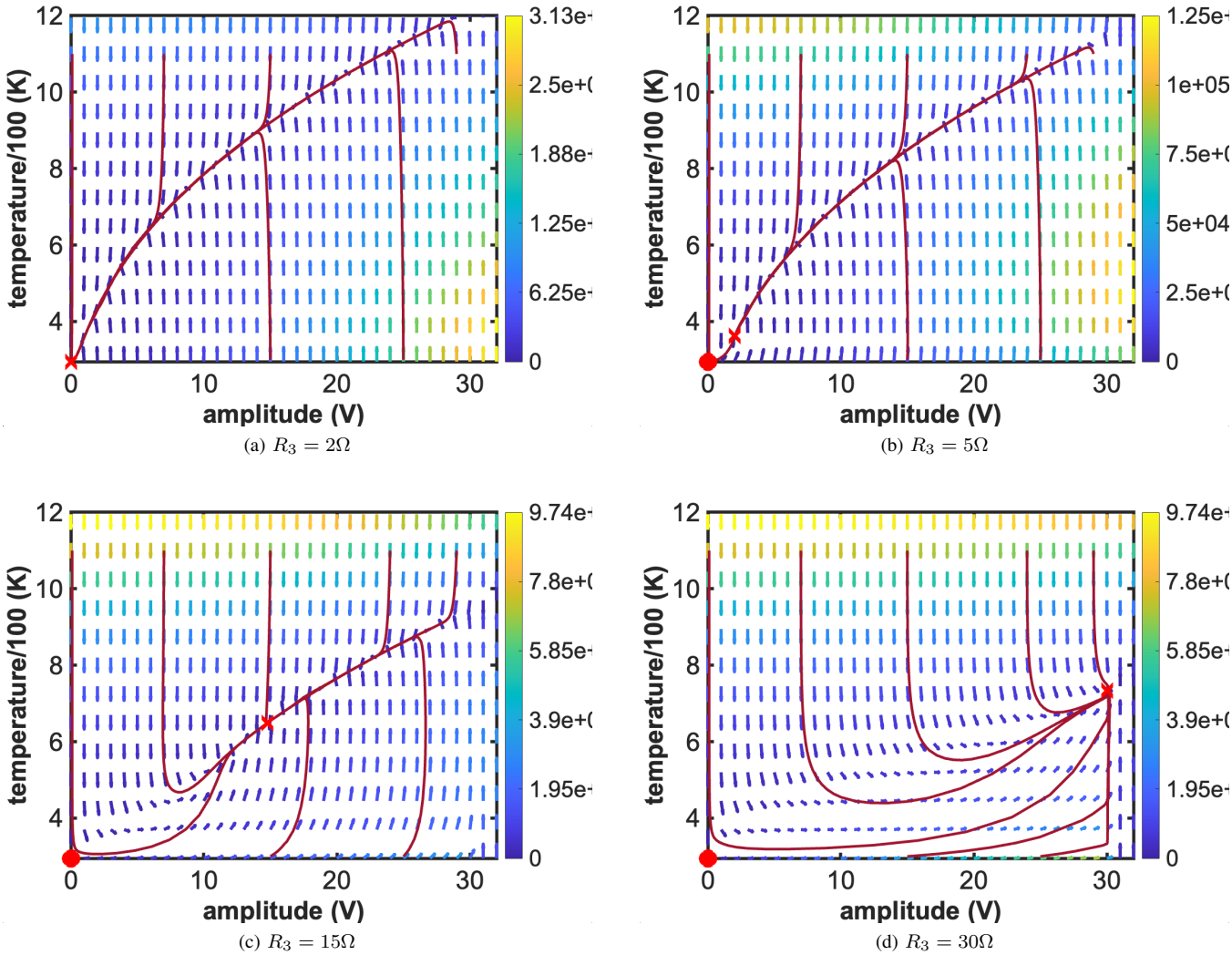

(a) $R_3 = 2\Omega$ (b) $R_3 = 5\Omega$

(c) $R_3 = 15\Omega$ (d) $R_3 = 30\Omega$

Fig. 13: Phase portraits for different values of R_3. Stable fixed point shown as red x, unstable shown as red circle.

$A = 25.88V$. The constructed version of this circuit is shown in Fig 15.

The time series data is shown in Fig 16, again collected using scope averaging. As we can see, our frequency measurement is still incredibly precise, and our amplitude estimate is quite accurate.

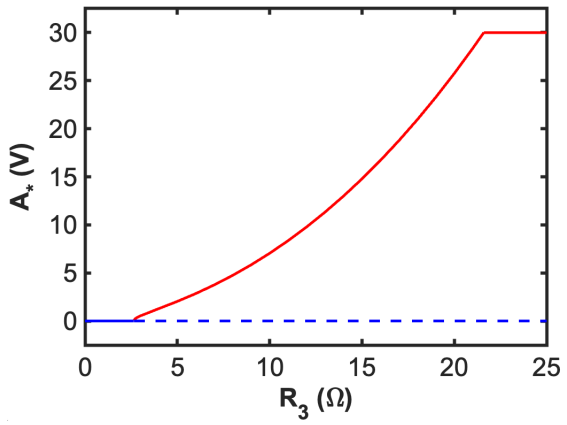

Fig. 14: Bifurcation diagram representing the A component of fixed points vs. R_3.

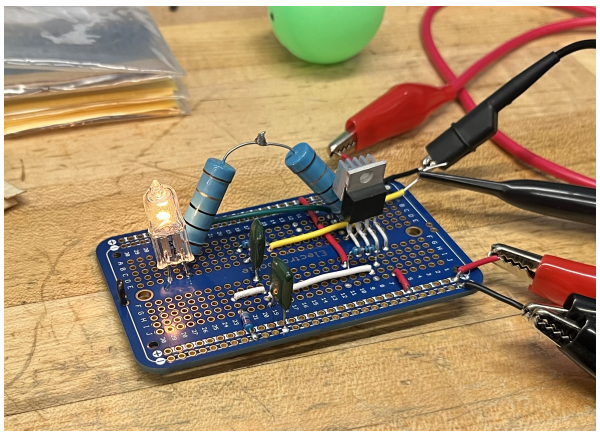

Fig. 15: Constructed version of the Wein bridge oscillator with lightbulb-driven nonlinear feedback.

V. Conclusion

The Wein bridge oscillator is one of the first oscillator circuits that was capable of generating low-distortion sinusoids of tunable amplitude. While sinusoids are a core part of linear systems analysis, we know that generating an isolated orbit requires a nonlinearity. In this report, we explored how both the unintentional nonlinearity of op-amp saturation and intentional nonlinearity that comes from temperature-dependent resistance in the feedback path can lead towards stable, sinusoidal oscillations.

Future research could explore using diodes as a (significantly more nonlinear) mechanism of nonlinear feedback for the Wein bridge oscillators. Diodes produce distortions that can be characterized with careful modelling. Additionally, there are other op-amp oscillator types; for example: phase shift oscillators, quadrature oscillators, Bubba oscillators [2]. These all use different linear circuit structures and nonlinearities that enable fixed oscillations, each having their own interesting set of over nonlinear dynamics and qualitative behavior.

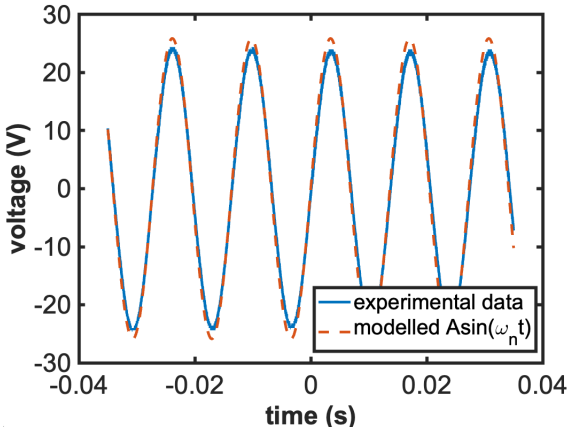

Fig. 16: Averaged time-series data taken on the Wein bridge oscillator circuit using lightbulb-driven nonlinear feedback.

VI. Acknowledgements

I'd like to thank Prof. Jörn Dunkel for teaching the class in such a clear, engaging manner.

References

[1] Harlow, D. (Fall 2019), MIT 8.022 Lecture Notes.
[2] Texas Instruments (2008). "Design of op-amp oscillators." https://www.ti.com/sc/docs/apps/msp/journal/aug2000/aug_07.pdf
[3] Lang, J. H. (Spring 2020), MIT 6.002 Lecture Notes.
[4] Trumper, D. L. (Spring 2022), MIT 2.14 Lecture Notes.
[5] Texas Instruments. "HANDBOOK OF OPERATIONAL AMPLIFIER APPLICATIONS." https://www.ti.com/lit/an/sboa092b/sboa092b.pdf?ts=1714681961383
[6] Meacham, L. A. (October 1938), "The Bridge Stabilized Oscillator", Bell System Technical Journal, 17 (4): 574–591, doi:10.1002/j.1538-7305.1938.tb00799.x.
[7] HyperPhysics. "Temperature Coefficient of Resistance." http://hyperphysics.phy-astr.gsu.edu/hbase/electric/restmp.html.
[8] Hosoi, A. P et al (Fall 2021). MIT 2.005 Lecture Notes.